CLM-R 37

United Kingdom Atomic Energy Authority

RESEARCH GROUP

Report

A SINGLE LOOP CONDUCTOR FOR PRODUCING A MAGNETIC WELL

F. M. LARKIN

Culham Laboratory,

Culham, Abingdon, Berkshire

1964

Available from H. M. Stationery Office

TWO SHILLINGS AND SIXPENCE NET

U.D.C.
621.039 : 634 : 538.122
621.039 : 624

UNCLASSIFIED
(Approved for sale)

CLM - R 37

A SINGLE LOOP CONDUCTOR FOR PRODUCING A MAGNETIC WELL

by

F.M. LARKIN

A B S T R A C T

The report describes a single loop conductor, shaped like the seam on a tennis ball, which generates the simplest type of magnetic well. Some contours of constant field strength are presented, for a number of variations on the standard case, which illustrate the possible range of mirror ratios. Also a preliminary study indicates that an efficiency of at least 60% may be achieved in the Lorentz trapping of injected neutral atoms.

U.K.A.E.A. Research Group,
Culham Laboratory,
Nr. Abingdon,
Berks.

June, 1964 (C 18 ED)

C O N T E N T S

1. INTRODUCTION

1. Recent interest in magnetic fields having a local minimum in field strength, as possible containers of plasma, has stimulated investigation into the types of conductor configuration which will produce such "magnetic wells". M.S. Ioffe et al.[1] originally suggested the addition of a linear, axial cusp to a simple mirror and J. Andreoletti[2] has studied a number of other magnetic well configurations. J.B. Taylor[3] has shown that point minima in magnetic fields may be classified by the order of the highest non-zero derivatives of φ, where the field $\underline{B}$ is given by:-

$$\underline{B} = -\nabla\varphi , \qquad \ldots (1)$$

and that the possible shape of a magnetic flux tube near such a minimum is rather limited. Andreoletti has also pointed out that the simplest (and most common) flux tube which has a minimum in $|\underline{B}|$ at the centre of a circular cross-section has elliptic cross-sections on either side of the circular one, with the major axes of these ellipses inclined at right angles. In view of the limited number of possible point minima it is natural to ask what is the simplest type of conductor configuration which can produce this simplest type of point minimum in field strength.

2. This report describes a conductor in the form of a single, closed loop, which generates a magnetic field with the basic type of point minimum and also possesses some other geometric properties which appear to be advantageous from a practical point of view. This conductor is simple, geometrically and topologically, (although of course the ultimate criterion of simplicity is generally production cost for a given result, which cannot be discussed here).

2. DESIRABLE FEATURES IN A MAGNETIC WELL

3. For the purpose of plasma containment a magnetic well should satisfy a number of practical requirements, and among these the following may be listed:-

(i) The well should be deep and have a reasonably large volume.

(ii) At the minimum of the well the magnetic field strength should still be large enough to ensure that the motion of contained particles is adiabatic.

(iii) The electric current required to maintain the field must not be prohibitively large.

(iv) Electromagnetic forces acting on the conductors should be as small as is practicable.

(v) Geometry of the conductors should be such as to allow convenient access to the magnetic well for plasma injection apparatus, diagnostic equipment, etc.

4. These requirements are highly interdependent and it is clear that some kind of compromise will have to be adopted in any practical design. One such compromise is discussed below and a preliminary attempt has been made to optimise on conditions (i), (ii) and (iii) within the limits of a filamentary conductor satisfying condition (v). Condition (iv) would have to be the subject of a detailed design study, but no special difficulties appear to exist which do not arise during the mechanical design of any other conductor carrying a large electric current.

3. A CONDUCTOR WITH CUBIC SYMMETRY

5. One way of producing a magnetic well is to combine a simple mirror field and two simple cusp fields, with the axes of the three systems mutually perpendicular and the three centres coincident. Fig.1 illustrates this arrangement using square loops for conductors. Clearly, as the square loops are moved together to form the edges of a cube some adjacent conductors reinforce each other while others nullify each other, and the limiting case can be simplified to one single loop which is shown in Fig.2. Contours of constant magnetic field strength are given in Figs.3 and 4 and these do illustrate the presence of a magnetic well. Fig.3 is a central plane normal to the mirror axis and Fig.4 is a central plane normal to one of the cusp axes. The corners of the figures lie in the edges of the cube which forms the conductor.

6. For a current of 1 MA in the conductor the field strength at the well minimum is 2.309 kG if the edge length of the cube is 2 m. The magnetic well is then enclosed by the surface defined by:-

$$|\underline{B}| \simeq 3.1 \text{ kG},$$

giving a perimeter/centre mirror ratio of about 1.35.

4. A "TENNIS BALL SEAM" CONDUCTOR CONFIGURATION

7. In attempting to improve on the "cube edge" conductor configuration one is led to consider the effect of rounding off the corners of the cube. The object of this is two-fold:

(i) to reduce that fraction of the volume contained by the conductor which is not part of the magnetic well, thus increasing the efficiency of the magnetic field design; and

(ii) to increase the height of the magnetic well by forcing the conductor nearer to weak spots in the wall of the well.

8. A consequence of rounding the corners can be a weakening of the mirror part of the magnetic field, thus decreasing the field strength at the well minimum and increasing the mirror ratio. Weakening the minimum field strength can be tolerated provided it is not overdone and, provided the motion of trapped particles remains adiabatic at the well minimum, increasing the mirror ratio will be advantageous.

9. This process of rounding off the corners of the cube results in a closed loop which is reminiscent of the shape of the seam on a tennis ball. One parametric expression which could be used to characterise such a curve is:-

$$
\begin{aligned}
x &= \lambda.\{\, a.\mathrm{Cos}(\theta + {}^{\pi}/_{4}) - b.\mathrm{Cos}\ 3\ (\theta + {}^{\pi}/_{4})\} \\
y &= \mu.\{\, a.\mathrm{Sin}(\theta + {}^{\pi}/_{4}) + b.\mathrm{Sin}\ 3\ (\theta + {}^{\pi}/_{4})\} \qquad \ldots (2) \\
z &= c.\mathrm{Sin}\ 2\theta, \quad 0 \leqslant \theta < 2\pi,
\end{aligned}
$$

a, b, c are constants.

Eliminating the parameter θ we find:-

$$\frac{x^2}{\lambda^2} + \frac{y^2}{\mu^2} + \frac{4ab}{c^2}\,.\,z^2 = (a+b)^2\ , \qquad \ldots (3)$$

so that if λ and μ are constant the space curve lies in the surface of an ellipsoid. However, the case where λ and μ depend on z may be of interest so we set:-

$$
\begin{aligned}
\lambda &= 1 + d.\mathrm{Sin}2\theta = 1 + \frac{d.z}{c} \\
\mu &= 1 - d.\mathrm{Sin}2\theta = 1 - \frac{d.z}{c}\ ,
\end{aligned}
\qquad \ldots (4)
$$

10. The cross-section, perpendicular to the z axis, through the surface defined by (3) is then an ellipse whose semi-axes are given by the expressions:-

$$\left(1 + \frac{d.z}{c}\right).\left\{(a+b)^2 - \frac{4ab}{c^2}\,.\,z^2\right\}^{\frac{1}{2}} \quad \text{and} \quad \left(1 - \frac{d.z}{c}\right).\left\{(a+b)^2 - \frac{4ab}{c^2}\,.\,z^2\right\}^{\frac{1}{2}} \ \ldots (5)$$

Fig.5 shows the projection, onto the plane $z = 0$, of a space curve of the type described by equation (2), with $a = \frac{3}{4}$, $b = \frac{1}{4}$, $d = 0$.

11. The magnetic field generated by a typical "tennis ball seam" conductor is illustrated in Fig.6. This shows the spatial relationship between the conductor and a resultant sheaf of field lines which form a magnetic well of the simplest type. One can see intuitively from the photograph that a "tennis ball seam" type of curve is the simplest form of filamentary, single loop conductor which can be "wrapped around" a magnetic well of the type considered in order to generate it.

5. EFFECTS OF VARYING THE PARAMETERS

12. Contours of constant field strength have been drawn for a variety of values of the parameters a, b, c and d, and are shown in Figs.7 to 22. In all cases presented the value $(a+b)$, which represents the radius of the circumcircle in the plane $z = 0$, has been set equal to unity. If $(a+b)$ is regarded as being 1 m. and the unit current in the conductor as 1 MA the contour heights marked 1, 2, 3 etc. may be regarded as representing 1 kG, 2 kG, 3 kG, etc. For any other values of radius and current the magnetic field strength will scale in proportion to $\frac{\text{current}}{\text{length}}$.

13. The "standard case" is $a = \frac{3}{4}$, $b = \frac{1}{4}$, $c = \sqrt{3}/2$, $d = 0$ which results in a space curve, lying in the surface of a sphere of radius 1, whose tangents at the four points of intersection with the plane $z = 0$ are all normal to that plane. Keeping $(a+b)$ equal to 1 the values $(a-b)$, c and d have been varied separately about these standard values. Table 1 below lists the effect of this parameter variation on the field strength, B_0, at the well minimum and B_1, the height of the constant field strength surface which forms the boundary of the magnetic well. The approximate volume of the well may be judged from the appropriate diagrams, whose numbers are also listed in the table. Note that in comparing well volumes one must remember that the volume of surface (3) also varies from case to case.

TABLE 1

$a + b = 1$ m; current = 1 MA

	metres			kG			
Case Number	$a - b$	c	d	B_0	B_1	B_1/B_0	Figure Numbers
1	½	$\sqrt{3}/2$	0	2.439	5.23	2.15	7, 8
2	¼	$\sqrt{3}/2$	0	0.134	5.71	42.7	9, 10
3	¾	$\sqrt{3}/2$	0	3.644	4.13	1.13	11, 12
4	½	1	0	1.903	5.13	2.70	13, 14
5	½	$\sqrt{3}-1$	0	3.180	5.42	1.71	15, 16
6	½	$\sqrt{3}/2$	⅓	0.554	5.64	10.04	17, 18
7	½	$\sqrt{3}/2$	-⅓	3.730	4.30	1.15	19, 20
8	½	0.65	⅓	1.930	5.89	3.05	21, 22

14. From Table 1 we see that the principal effect of varying the parameters is to alter the mirror part of the total field. The value of B_o is more sensitive to changes in a, b, c and d than is B_1, the height of the well wall. One can now choose any of a large number of "optimal" forms and as an example suppose that B_o is required to be about 2.0 and B_1/B_o at least 3.0. We notice that decreasing c (case 5) and increasing d (case 6) have opposite effects on the value of B_o, and both tend to increase B_1. Case 8 in the table represents the result of decreasing c and increasing d to produce a roughly spherical magnetic well which goes some way to meeting the conditions stipulated in section 2.

6. LORENTZ TRAPPING

15. One must, of course, consider ways and means of getting plasma into the magnetic well and, in order to give an example, the method of Lorentz trapping will be considered here. Fig.23 shows the variation of $|\underline{V} \wedge \underline{B}|$ along various injection lines, where $\underline{V}$ is in fact a velocity of unit magnitude and $\underline{B}$ kG is the magnetic field due to the standard form of tennis ball seam (case 1 of Table 1). The injection lines are all assumed to lie in the plane $x = 0$ and to intersect the centre of the magnetic well, making different angles θ with the y axis. This injection geometry is illustrated in Fig.24.

16. Also indicated in Fig.23 are the angles, in radians, which the injection lines make with the y axis and the range of values of $|\underline{V} \wedge \underline{B}|$ within which the ionized particles are trapped in the magnetic well. The solid sections of the curves indicate values of $|\underline{V} \wedge \underline{B}|$ for which injected particles will be trapped. For example, on the injection line for which $\theta = 0.5$ radians any particles whose characteristic $|\underline{V} \wedge \underline{B}|$ lies between 1.8 and 3.65 will be both ionized and trapped. Particles whose characteristic $|\underline{V} \wedge \underline{B}|$ lies outside this range may or may not be ionized, but in any case they will not be trapped.

17. It appears from Fig.23 that trapping efficiency increases monotonically as the injection line approaches intersection with the conductor itself. However, in any real experiment the choice of injection angle would depend upon a number of practical considerations and, in particular, would not be allowed to intersect the conductor. In this example a reasonable compromise might be at $\theta = 0.7$ radians, on which particles with characteristic $|\underline{V} \wedge \underline{B}|$ between the values 1.7 and 4.3 will be trapped. Thus, if the injected particles have $|\underline{V} \wedge \underline{B}|$ roughly uniformly distributed between 0.0 and 4.3, a trapping efficiency of 60% could be achieved.

7. ACKNOWLEDGEMENT

18. The author is grateful to Mrs. B. King for help in computing some of the numerical results.

8. REFERENCES

1. GOTT, Yu.V., IOFFE, M.S. and TELKOVSKY, V.G. Some new results on confinement in magnetic traps (In Russian). Nuclear Fusion 1962 Supplement, Pt 3, pp.1045-1047, 1962.

2. ANDREOLETTI, J. Methods for systematic investigations of "magnetic pits" (In French). C.R. Acad. Sci., Paris, vol.257, pp.1235-1237, August 5, 1963.

3. TAYLOR, J.B. Culham Laboratory. Private communication.

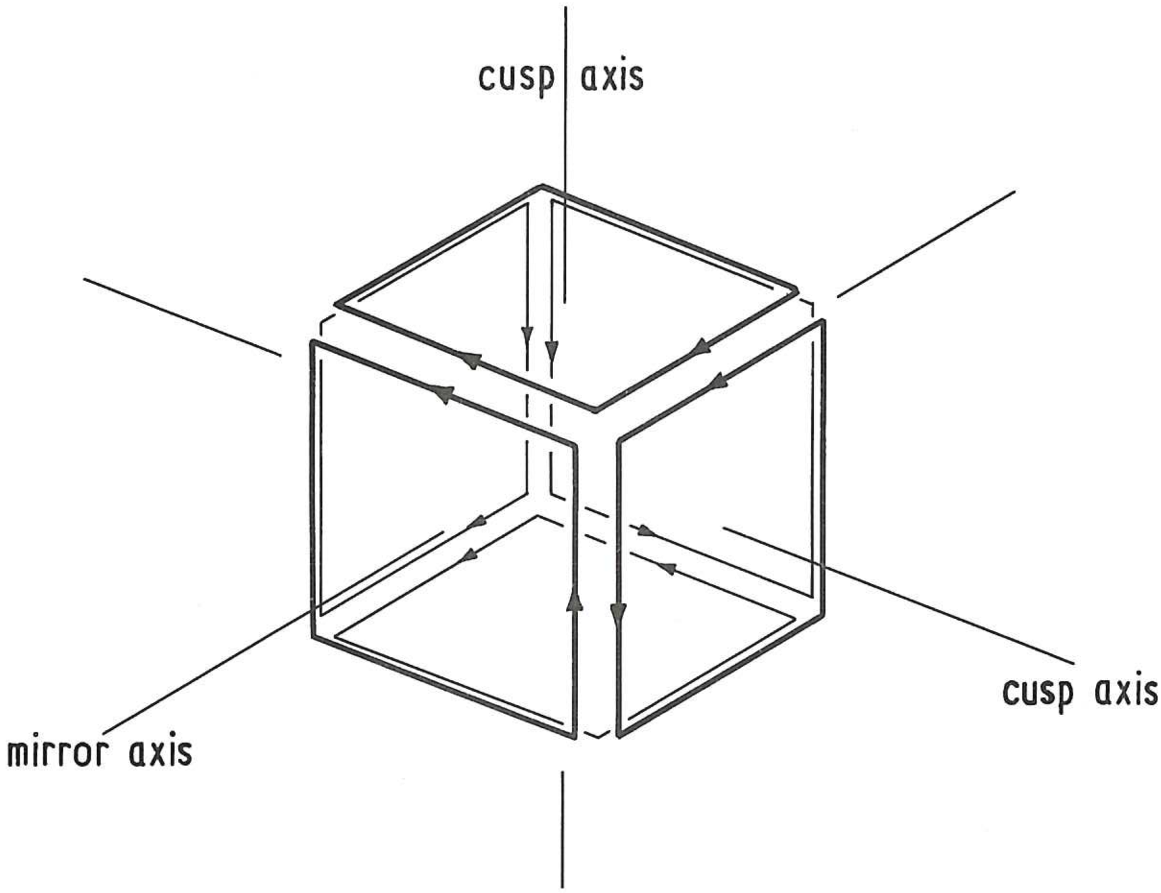

CLM-R 37 Fig. 1
A conductor arrangement which produces a combination of a magnetic mirror and two cusps, forming a magnetic well. (See para. 5)

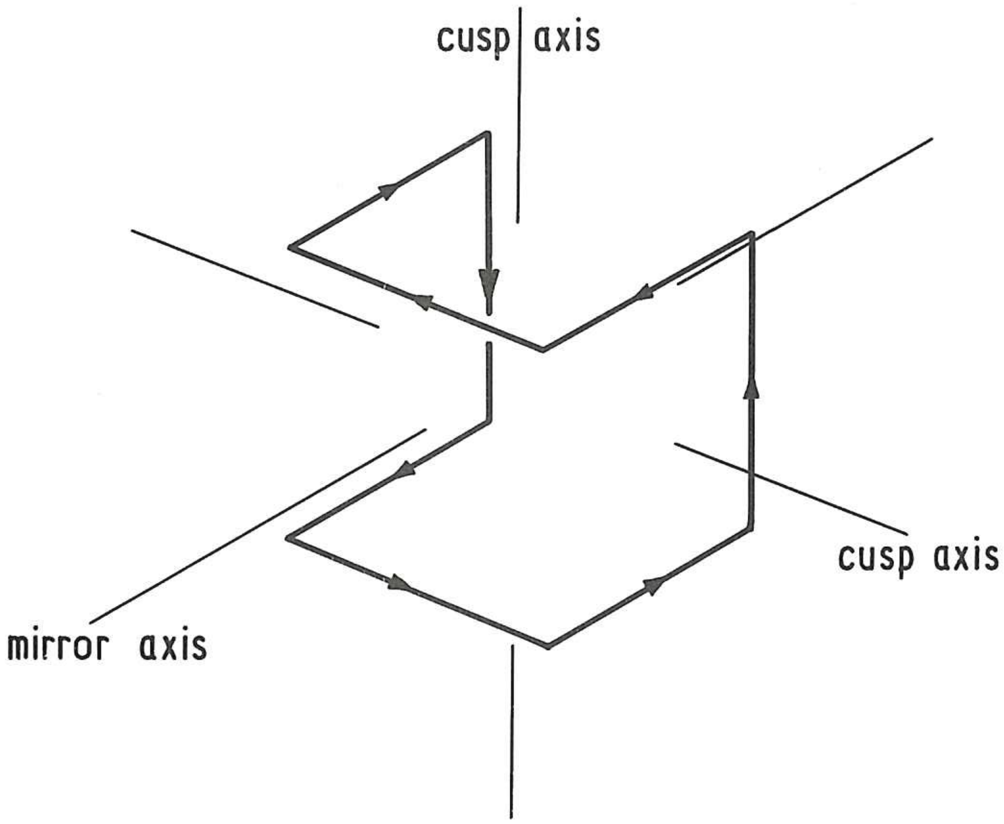

CLM-R 37 Fig. 2
A single loop conductor which generates the same magnetic well as the conductors in Fig. 1. (See para. 5)

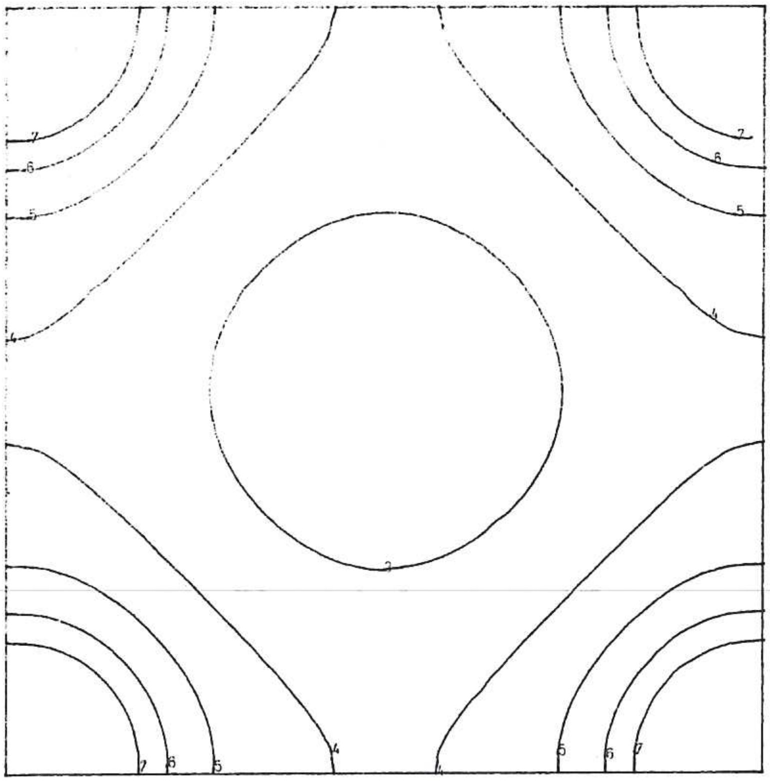

CLM-R 37 Fig. 3
Contours of constant $|\underline{B}|$ in a central plane normal to the mirror axis of the conductor illustrated in Fig. 2. (See para. 5)

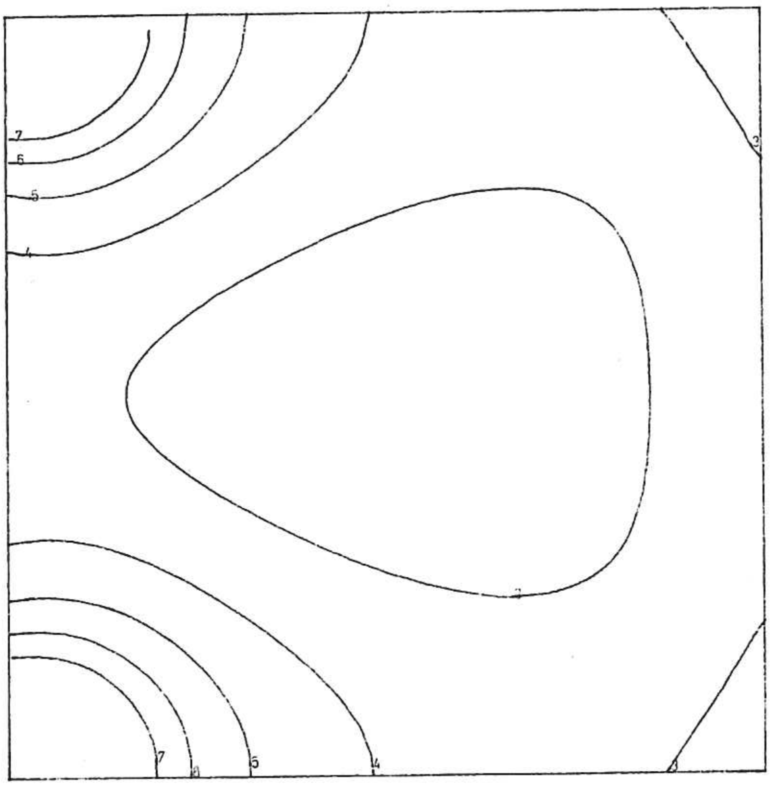

CLM-R 37 Fig. 4
Contours of constant $|\underline{B}|$ in a central plane normal to a cusp axis of the conductor illustrated in Fig. 2. (See para. 5)

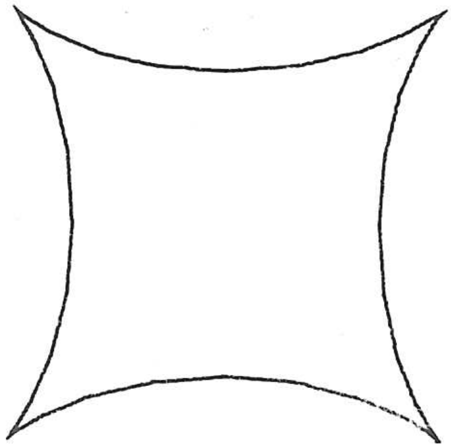

CLM-R 37 Fig. 5
Projection of a tennis ball seam type of conductor onto a plane normal to the mirror axis. (See para. 10)

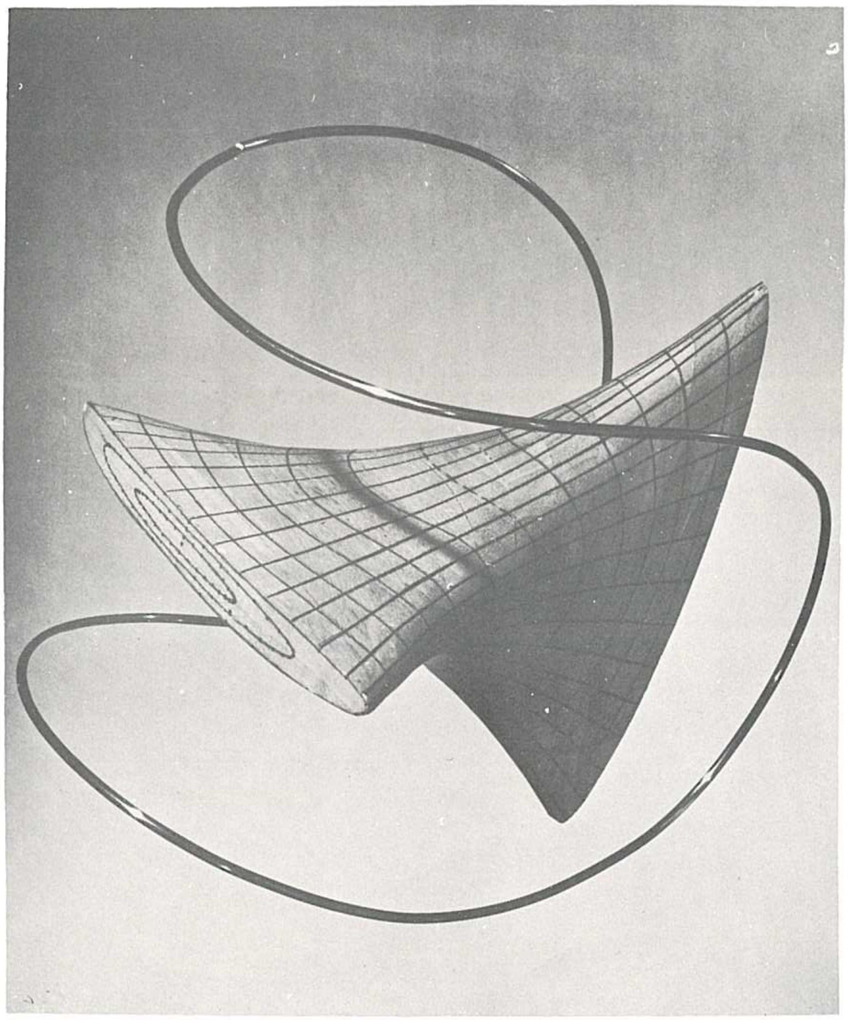

CLM-R 37 Fig. 6
Field lines associated with tennis ball seam conductor (See para. 11)

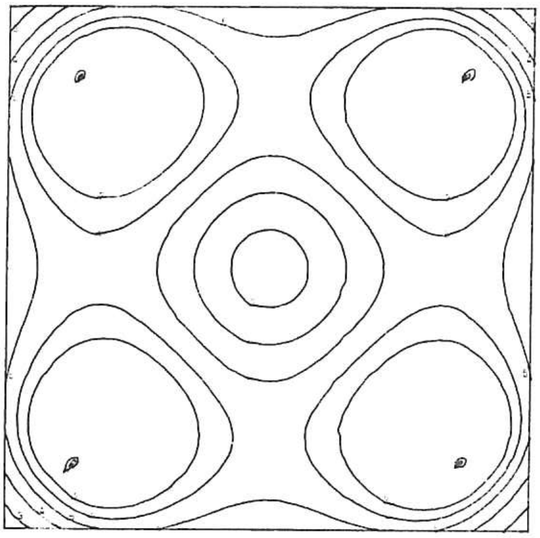

CLM - R 37 Fig. 7
Contours of constant $|\underline{B}|$ in a central plane normal to the mirror axis of tennis ball seam, case 1

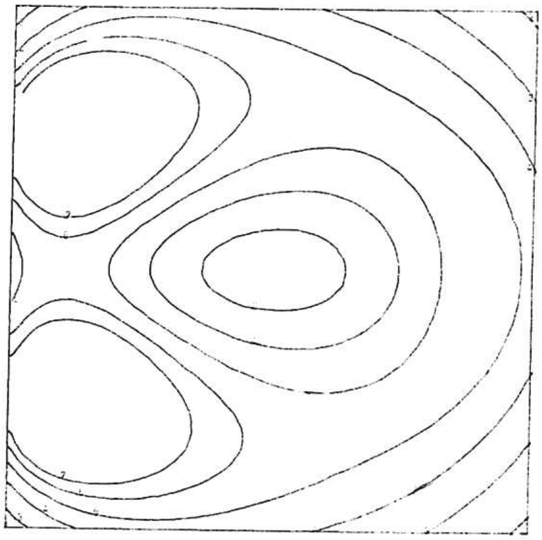

CLM - R 37 Fig. 8
Contours of constant $|\underline{B}|$ in a central plane normal to a cusp axis of tennis ball seam, case 1

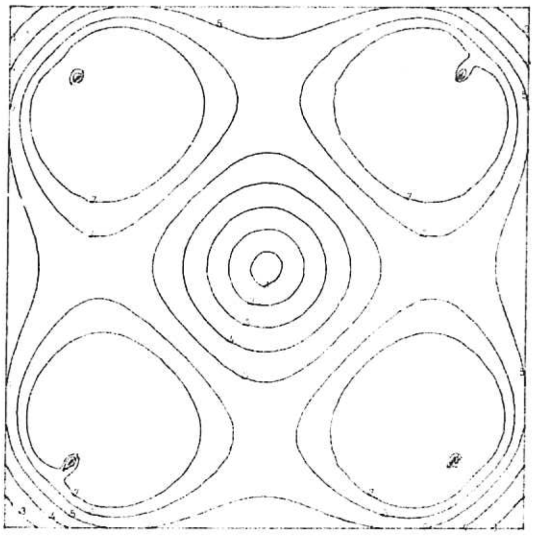

CLM - R 37 Fig. 9
Contours of constant $|\underline{B}|$ in a central plane normal to the mirror axis of tennis ball seam, case 2

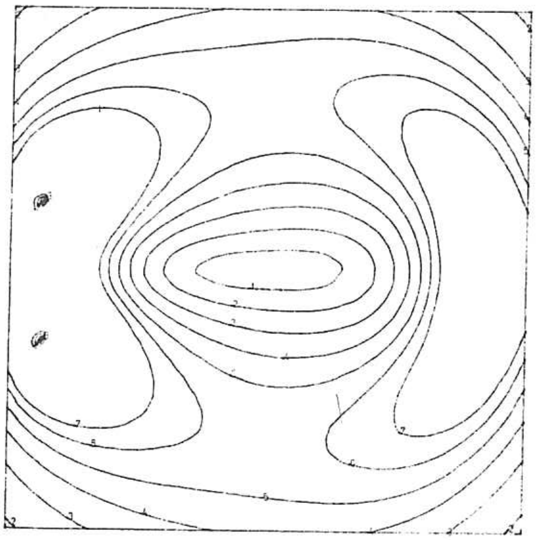

CLM - R 37 Fig. 10
Contours of constant $|\underline{B}|$ in a central plane normal to a cusp axis of tennis ball seam, case 2

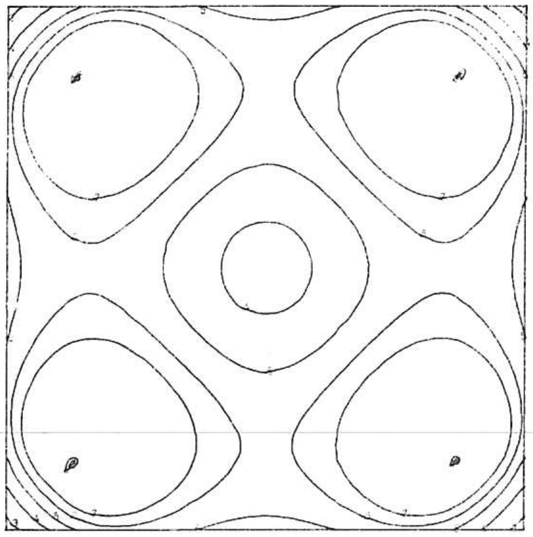

CLM - R 37 Fig. 11
Contours of constant $|\underline{B}|$ in a central plane normal to the mirror axis of tennis ball seam, case 3

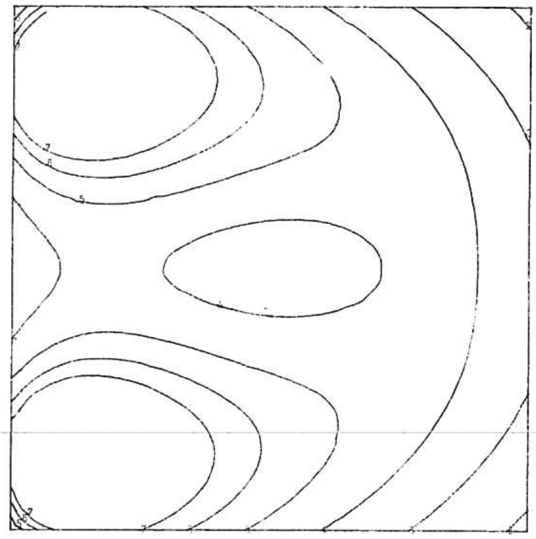

CLM - R 37 Fig. 12
Contours of constant $|\underline{B}|$ in a central plane normal to a cusp axis of tennis ball seam, case 3

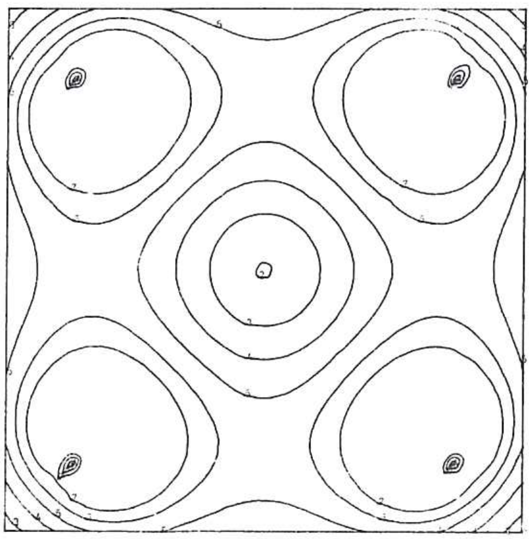

CLM - R 37 Fig. 13
Contours of constant $|\underline{B}|$ in a central plane normal to the mirror axis of tennis ball seam, case 4

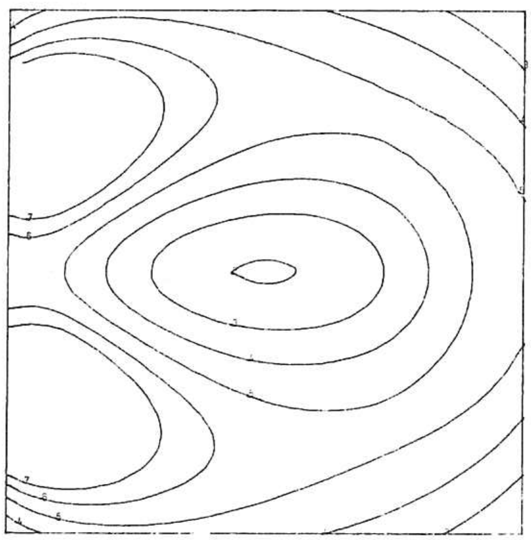

CLM - R 37 Fig. 14
Contours of constant $|\underline{B}|$ in a central plane normal to a cusp axis of tennis ball seam, case 4

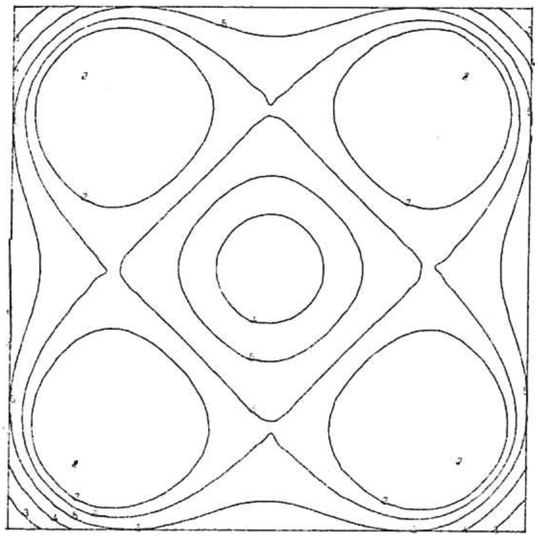

CLM - R 37 Fig. 15
Contours of constant $|\underline{B}|$ in a central plane normal to the mirror axis of tennis ball seam, case 5

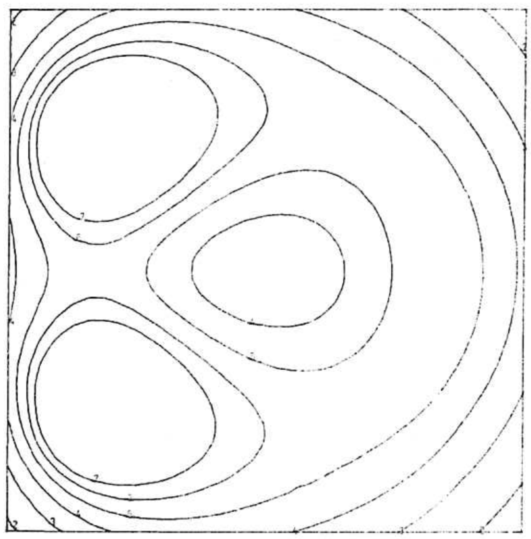

CLM - R 37 Fig. 16
Contours of constant $|\underline{B}|$ in a central plane normal to a cusp axis of tennis ball seam, case 5

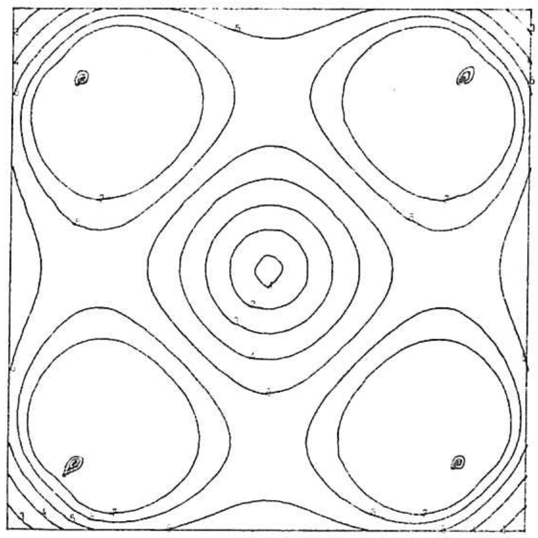

CLM - R 37 Fig. 17
Contours of constant $|\underline{B}|$ in a central plane normal to the mirror axis of tennis ball seam, case 6

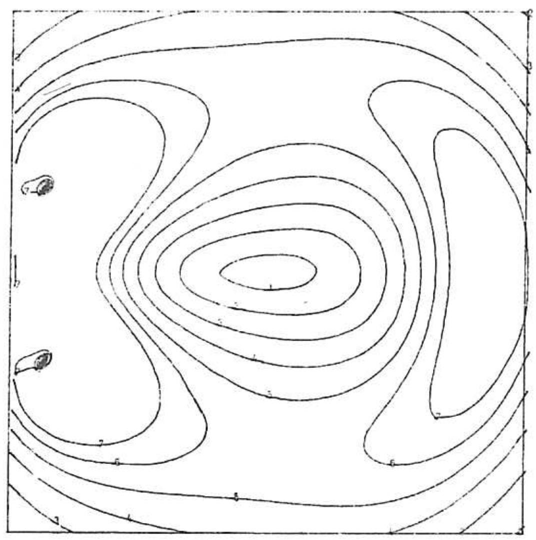

CLM - R 37 Fig. 18
Contours of constant $|\underline{B}|$ in a central plane normal to a cusp axis of tennis ball seam, case 6

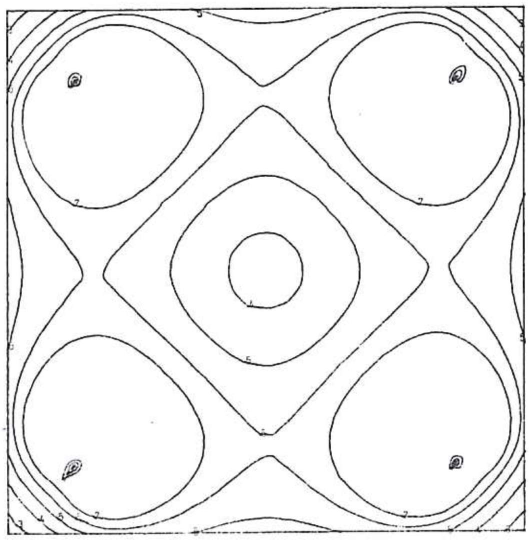

CLM-R37 Fig. 19
Contours of constant $|\underline{B}|$ in a central plane normal to the mirror axis of tennis ball seam, case 7

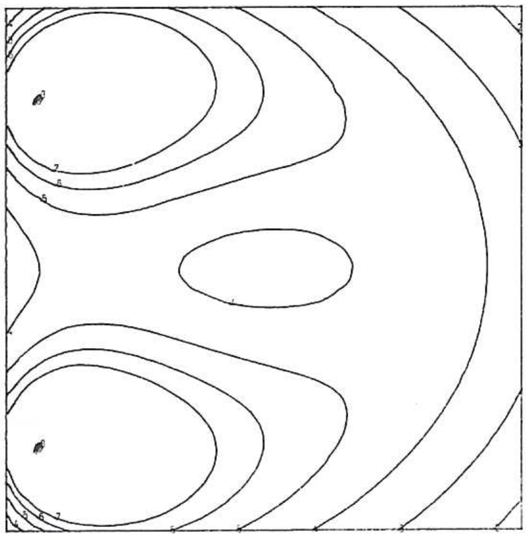

CLM-R37 Fig. 20
Contours of constant $|\underline{B}|$ in a central plane normal to a cusp axis of tennis ball seam, case 7

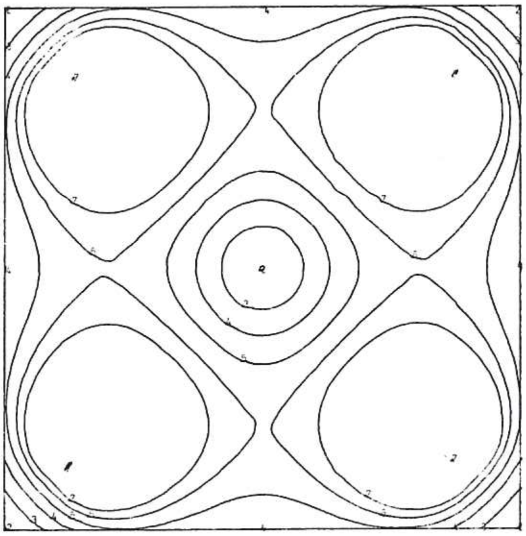

CLM-R37 Fig. 21
Contours of constant $|\underline{B}|$ in a central plane normal to the mirror axis of tennis ball seam, case 8

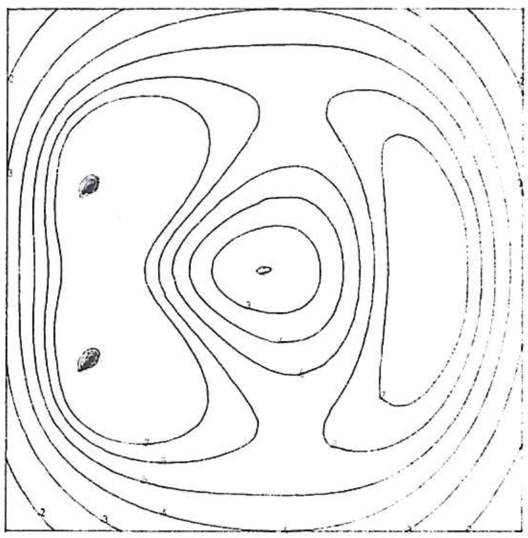

CLM-R37 Fig. 22
Contours of constant $|\underline{B}|$ in a central plane normal to a cusp axis of tennis ball seam, case 8

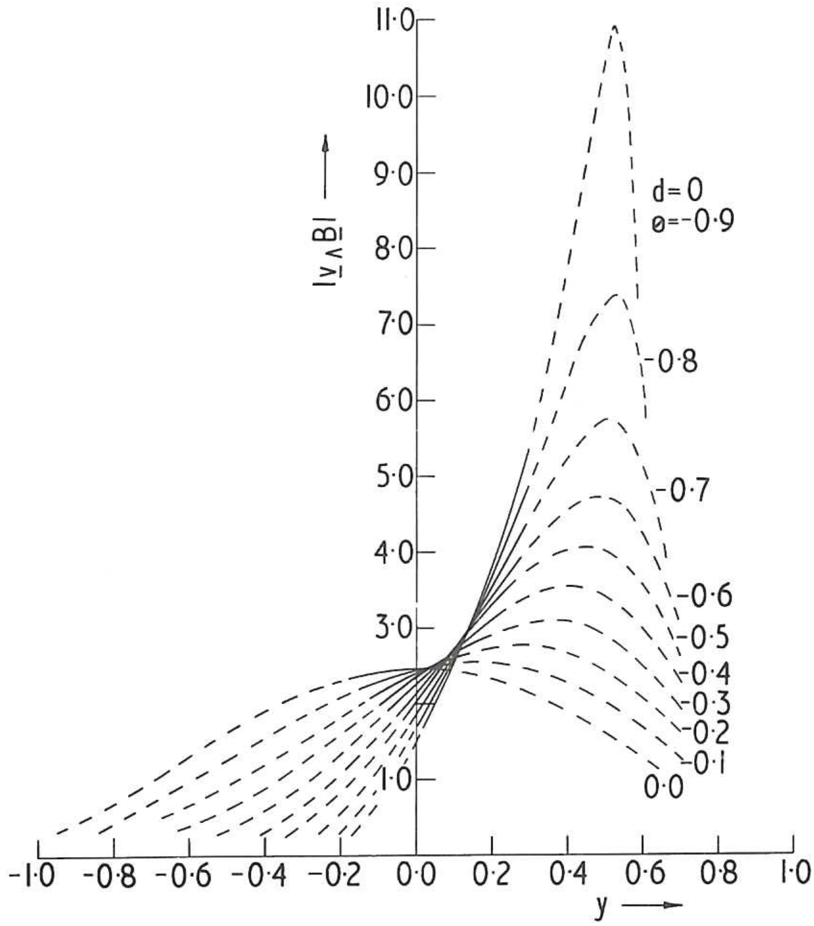

CLM-R 37 Fig. 23
The variation along various injection lines of the Lorentz force experienced by a neutral atom passing through a magnetic well. (See para. 15)

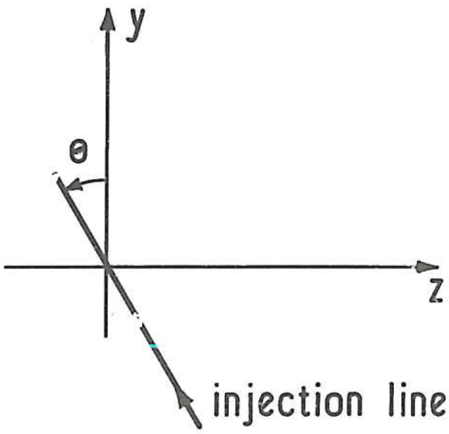

CLM-R 37 Fig. 24
The injection geometry assumed in the Lorentz trapping calculations. (See para. 15)

Available from
HER MAJESTY'S STATIONERY OFFICE
York House, Kingsway, London W.C. 2
423 Oxford Street, London W. 1
13a Castle Street, Edinburgh 2
109 St. Mary Street, Cardiff
39 King Street, Manchester 2
50 Fairfax Street, Bristol 1
35 Smallbrook, Ringway, Birmingham 5
80 Chichester Street, Belfast
or through any bookseller.

Printed in England

S.O. Code No. 91-3-16-29